

2012

## Role of twin Cys-Xaa<sup>9</sup>-Cys motif cysteines in mitochondrial import of the cytochrome c oxidase biogenesis factor Cmc1

Deepa V. Dabir

Loyola Marymount University, [deepa.dabir@lmu.edu](mailto:deepa.dabir@lmu.edu)

Follow this and additional works at: [https://digitalcommons.lmu.edu/bio\\_fac](https://digitalcommons.lmu.edu/bio_fac)

 Part of the [Biology Commons](#)

---

### Recommended Citation

Bourens M, Dabir DV, Tienson HL, Sorokina I, Koehler CM, Barrientos A. Role of twin Cys-Xaa<sup>9</sup>-Cys motif cysteines in mitochondrial import of the cytochrome C oxidase biogenesis factor Cmc1. *J Biol Chem.* 2012 Sep 7;287(37):31258-69. doi: 10.1074/jbc.M112.383562. Epub 2012 Jul 5. PMID: 22767599; PMCID: PMC3438957.

This Article is brought to you for free and open access by the Biology at Digital Commons @ Loyola Marymount University and Loyola Law School. It has been accepted for inclusion in Biology Faculty Works by an authorized administrator of Digital Commons@Loyola Marymount University and Loyola Law School. For more information, please contact [digitalcommons@lmu.edu](mailto:digitalcommons@lmu.edu).

# Role of Twin Cys-Xaa<sub>9</sub>-Cys Motif Cysteines in Mitochondrial Import of the Cytochrome *c* Oxidase Biogenesis Factor Cmc1\*

Received for publication, May 18, 2012, and in revised form, July 2, 2012. Published, JBC Papers in Press, July 5, 2012, DOI 10.1074/jbc.M112.383562

Myriam Bourens<sup>‡</sup>, Deepa V. Dabir<sup>§</sup>, Heather L. Tienson<sup>§</sup>, Irina Sorokina<sup>¶</sup>, Carla M. Koehler<sup>§</sup>, and Antoni Barrientos<sup>‡||1</sup>

From the Departments of <sup>¶</sup>Biochemistry & Molecular Biology and <sup>‡</sup>Neurology, University of Miami Miller School of Medicine, Miami, Florida 33136, the <sup>§</sup>Department of Chemistry and Biochemistry, UCLA, Los Angeles, California 90095, and <sup>¶</sup>Midwest Bio Services, LLC, Overland Park, Kansas 66211

**Background:** The Mia40-Erv1 import machinery facilitates oxidative folding of mitochondrial intermembrane space twin CX<sub>9</sub>C proteins such as Cmc1.

**Results:** Mutations in Cmc1 cysteines impair its oxidative folding and import.

**Conclusion:** Although *in vitro* excess Mia40 oxidizes Cmc1, *in vivo* Cmc1-Mia40-Erv1 form a ternary complex where Cmc1 oxidation may occur.

**Significance:** This mechanism may facilitate efficient formation of multiple disulfides.

The Mia40 import pathway facilitates the import and oxidative folding of cysteine-rich protein substrates into the mitochondrial intermembrane space. Here we describe the *in vitro* and *in organello* oxidative folding of Cmc1, a twin CX<sub>9</sub>C-containing substrate, which contains an unpaired cysteine. *In vitro*, Cmc1 can be oxidized by the import receptor Mia40 alone when in excess or at a lower rate by only the sulfhydryl oxidase Erv1. However, physiological and efficient Cmc1 oxidation requires Erv1 and Mia40. Cmc1 forms a stable intermediate with Mia40 and is released from this interaction in the presence of Erv1. The three proteins are shown to form a ternary complex in mitochondria. Our results suggest that this mechanism facilitates efficient formation of multiple disulfides and prevents the formation of non-native disulfide bonds.

Mitochondrial proteins are derived from a dual genetic origin with only a handful of proteins encoded in the mitochondrial genome and the vast majority encoded in nuclear genes. With such a large number of proteins derived from outside the mitochondria, cells have devised several mechanisms that allow for delivery of substrates to the organelle and to the correct suborganellar compartments (1). In particular, several pathways are used to import proteins into the mitochondrial intermembrane space (IMS)<sup>2</sup> with a small fraction utilizing a disulfide relay system that involves the import receptor Mia40 (2–4).

The Mia40 import pathway mirrors other disulfide-generating pathways including the protein-disulfide isomerase pathway of the endoplasmic reticulum and the Dsb pathway of the

bacterial periplasmic space (5, 6). The Mia40 pathway consists of the newly imported peptides, Mia40 and the sulfhydryl oxidase Erv1. The function of this pathway is to transfer both the formation of disulfide bonds to the newly imported substrates and reducing power to a final electron acceptor (6). Most import substrates in the Mia40 pathway contain one of two motifs, twin CX<sub>9</sub>C or CX<sub>3</sub>C. The twin CX<sub>9</sub>C motif is present in several small proteins involved in the assembly of cytochrome *c* oxidase (*e.g.*, Cox17, Cox19, Cmc1, and Cmc2 (7–9)), whereas twin CX<sub>3</sub>C-containing proteins include the small TIM proteins (*e.g.*, Tim13) (10), which facilitate the import of membrane proteins through the IMS. The twin CX<sub>9</sub>C motif consists of a coiled coil helix turn coiled coil helix structure, which is held together by disulfide bonds between the first and fourth cysteines and the second and third cysteines (7).

The Mia40 import pathway has been reviewed elsewhere (5, 11, 12). In brief, fully reduced import substrates pass through the TOM complex and enter the IMS where they interact with oxidized Mia40. For the small Tim proteins, the first cysteine in the CX<sub>3</sub>C motifs facilitates covalent binding of the substrate to Mia40 (13, 14). The import substrate folds, becomes oxidized, and is released from Mia40. This results in a reduced Mia40, which is reset into an oxidized form by Erv1 (4), through a direct functional interaction (15) involving hydrophobicity-driven binding of the Erv1 N-terminal domain to the Mia40 substrate binding cleft to facilitate efficient electron transfer (16). Subsequently, Erv1, directly or through the action of cytochrome *c* and cytochrome *c* oxidase, delivers electrons to oxygen, thus regenerating itself to become competent for another round of interaction with reduced Mia40 (17–19). The steps involved in full oxidation of the import substrates and their release in a folded conformation remain to be fully understood (12).

Based on *in vitro* reconstitution assays, a recent report proposed scenarios involving oxidation of the twin CX<sub>9</sub>C protein Cox19 by an excess of Mia40, which is further enhanced by the presence of glutathione (20). However, for CX<sub>3</sub>C-containing Tim proteins, a ternary complex of Erv1, Mia40, and imported substrate has been detected in mitochondria (21), and so a pos-

\* This work was supported, in whole or in part, by National Institutes of Health Grants GM071775A (to A. B.), GM061721 (to C. M. K.), GM07185 (to H. L. T.), and 1F32GM084568-01A1 (to D. V. D.). This work was also supported by a Muscular Dystrophy Association Research Grant (to A. B.).

<sup>1</sup> To whom correspondence should be addressed: Depts. of Neurology and Biochemistry & Molecular Biology, University of Miami Miller School of Medicine, 1600 NW 10th Ave., RMSB 2067, Miami, FL 33136. Tel.: 305-243-8683; Fax: 305-243-7404; E-mail: abarrientos@med.miami.edu.

<sup>2</sup> The abbreviations used are: IMS, intermembrane space; AMS, 4-acetamido-4'-maleimidylstilbene-2,2'-disulfonic acid; PK, proteinase K.

**TABLE 1**  
Genotype and source of yeast strains

Strain	Genotype	Source
W303	MATa <i>ade2-1 his3-1,15 leu2-3,112 trp1-1 ura3-1</i>	<sup>a</sup>
BY4741	MATa <i>his3Δ1 leu2Δ0 met15Δ0 ura3Δ0</i>	Ref. 23
BYΔ <i>cmc1</i>	MATa <i>his3Δ1 leu2Δ0 met15Δ0 ura3Δ0 CMC1::KANX</i>	Ref. 23
<i>erv1-101</i>	MATα <i>his311,15 leu2 ura3 trp1 ade8 erv1::HIS3[perv1-101:TRP1 CEN]</i>	Ref. 17
<i>mia40-3</i>	MATa <i>ade2-101 his3-200 leu2-1 ura3-52 trp1-63 lys2-80 mia40::ADE2 (pFL39-FOMP2-8ts/mia40-3)</i>	Ref. 2
<i>mia40-4</i>	MATa <i>ade2-101 his3-200 leu2-1 ura3-52 trp1-63 lys2-80 mia40::ADE2 (pFL39-FOMP2-7ts/mia40-4)</i>	Ref. 2

<sup>a</sup> Dr. R. Rothstein (Department of Human Genetics, Columbia University, New York, NY).

sible role for Erv1 in substrate oxidation has not been fully discarded.

Here we report the *in vitro* oxidative folding and *in organello* import of Cmc1, a twin CX<sub>9</sub>C-containing Mia40/Erv1 substrate, which contains an unpaired cysteine. *In vitro*, reduced Cmc1 can be oxidized by superstoichiometric amounts of Mia40 alone or slowly by even substoichiometric concentrations of Erv1 alone or cytochrome *c* alone. However, efficient *in vitro* Cmc1 oxidative folding and physiological *in organello* Cmc1 import require the cooperative action of Mia40 and Erv1. Mia40, Erv1, and Cmc1 are shown to form a ternary complex where substrate oxidation presumably occurs. This mechanism for oxidative folding in the IMS could serve to promote substrate channeling and minimize the formation of nonphysiological disulfide bonds.

## EXPERIMENTAL PROCEDURES

**Yeast Strains and Growth Conditions**—The strains carrying temperature-sensitive alleles of *MIA40* (*mia40-3* and *mia40-4*) (2) and *ERV1* (*erv1-101*) (17) in centromeric plasmids were previously reported. All of the *Saccharomyces cerevisiae* strains used are listed in Table 1. The growth media compositions have been described elsewhere (22).

**Mutational Analysis**—Wild-type and cysteine point mutant genes (C42A, C52A, C64A, C74A, and C104A) of *CMC1* were cloned in a multicopy plasmid (pYEplac181) and transformed into the previously reported BY4741Δ*cmc1* strain (23). Mitochondria were isolated as reported (23), and a 50-μg sample was used for protein separation on 12% SDS-PAGE and immunoblotting for Cmc1.

**Reconstitution and Analysis of Trapped Thiols**—Purifications of recombinant wild-type and mutant forms of Cmc1, Erv1, and Mia40 were performed as stated elsewhere (8, 10, 17, 23). Recombinant Cmc1 or cysteine mutant proteins were reduced with 5 mM DTT for 1 h. DTT was removed by gel filtration using a NAP25 column, and Cmc1 was eluted in 20 mM Tris-HCl, pH 7.0, 150 mM KCl, and 0.1 mM EDTA as reported (10). For experiments using substoichiometric concentrations of Erv1/Mia40, substrate proteins at a concentration of 10 μM were mixed with 2 μM Erv1, 2 μM Mia40, or in combination. In some experiments, a 1–20-fold excess of Mia40 or Erv1 was used. In a set of experiments, oxidized cytochrome *c* was included at substoichiometric concentrations. Cmc1 was confirmed reduced at the start of the experiment by incubation with and without 4-acetamido-4'-maleimidylstilbene-2,2'-disulfonic acid (AMS) as described below. One AMS molecule will covalently bind to one reduced cysteine and result in a gel shift increase of ~500 daltons. For example, Cmc1 contains five cysteines, and if each cysteine is reduced, five AMS

molecules will bind and increase the molecular mass of the protein by ~2.5 kDa. The redox state of Cmc1 was indicated by thiol modification with AMS at varying time points (0–4 h) as indicated in the figures. To 15 μl of buffer as stated above, 5 μl of sample was added with the addition of 20 mM AMS and incubated at 37 °C for 1 h. The samples were separated on 12% SDS-PAGE gels followed by immunoblotting for Cmc1. Reconstitutions in the presence of cytochrome *c* were done as reported (20).

**Hydrogen Peroxide Assay**—In some reconstitution experiments with reduced Cmc1, the production of H<sub>2</sub>O<sub>2</sub> was measured using the Amplex Red hydrogen peroxide/peroxidase assay kit (Invitrogen) as reported (10) and according to the manufacturer's protocol.

**Mass Spectrometry**—Reconstitution of reduced Cmc1 was performed with Mia40 or in combination with Erv1 for 2 h and followed by protein separation on 12% SDS-PAGE. The gel was stained with Coomassie Blue, and the relevant bands were excised, dried, and analyzed for mass spectrometry. In-gel digests were performed by incubating the gel slices at 37 °C overnight with sequencing grade modified trypsin (Promega). The resulting peptide mixture was extracted from the gel and concentrated on the Captrap peptide trap (Michrom Bioresources) and separated on a BioBasic C18 PicoFrit microcapillary column (New Objective) by a 45-min gradient of 7–93% acetonitrile in water and 0.1% formic acid. Eluting peptides were electrosprayed directly into a DECA-XP Plus ion trap mass spectrometer equipped with a nano-LC electrospray ionization source (ThermoElectron). Full MS as well as tandem MS/MS spectra were recorded. BioWorks 3.2 software (ThermoElectron) based on SEQUEST algorithm was used for data analysis. The data were also analyzed by MassMatrix software developed by Hua Xu (University of Illinois) and Michael A. Freitas (The Ohio University Medical Center). The searches were performed in the National Institutes of Health nonredundant protein database, as well as the custom database containing the sequences of the overexpressed protein products. Peptide/spectra matches were retained if the following criteria were met: XCor scores higher than 1.5 for peptides charged +1, higher than 2.0 for peptides charged +2, and higher than 2.5 for peptides charged +3 and peptide probability lower than 0.05.

**In Organello Import of Radiolabeled Proteins into Mitochondria**—[<sup>35</sup>S]Methionine-labeled proteins were generated with TNT quick coupled transcription/translation kits (Promega) and plasmids carrying wild-type and cysteine variants of *CMC1*. Import reactions were conducted as reported (24).

Frozen mitochondria aliquots were thawed and added to the import buffer at a final concentration of 100 μg/ml. Following a

## Oxidative Folding of Cmc1

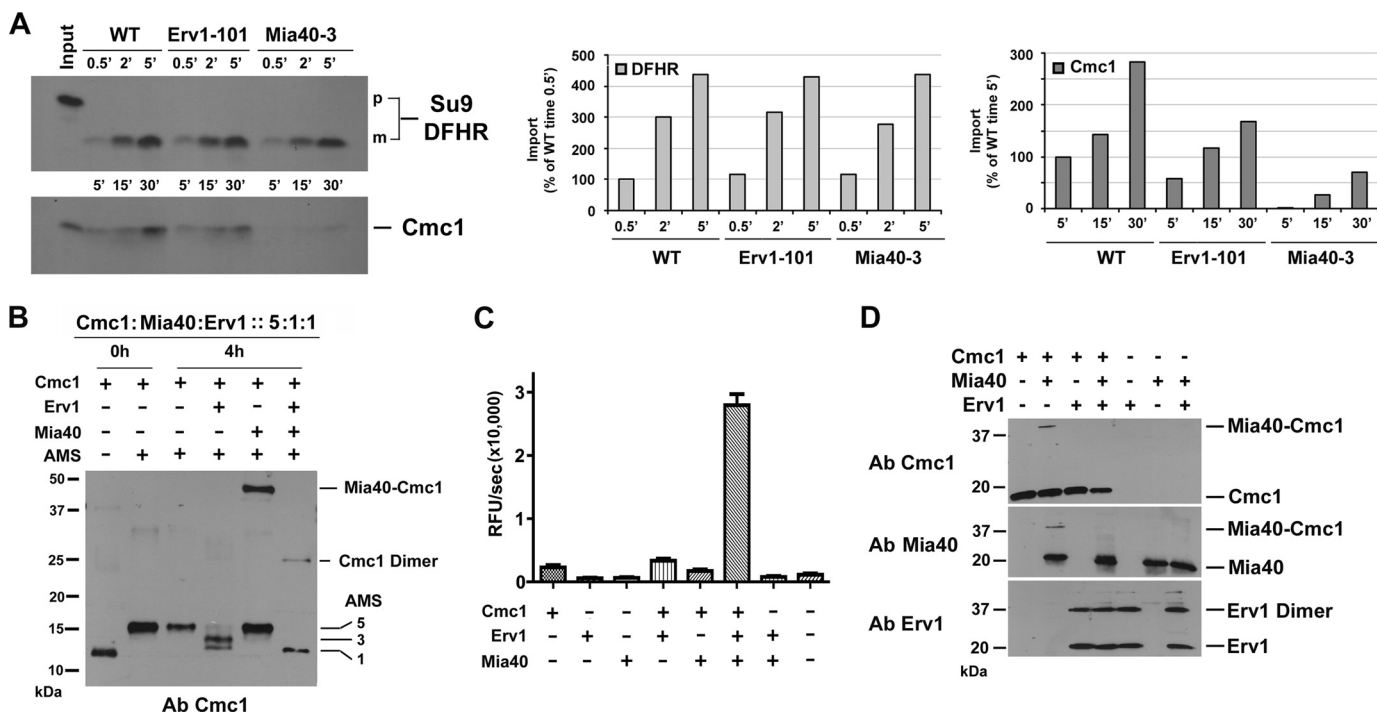


**FIGURE 1. Cmc1 is an Mia40-Erv1 pathway import substrate.** *A*, *in organello* mitochondrial protein import of *in vitro* synthesized wild-type  $^{35}\text{S}$ -labeled precursor Cmc1 into mitochondria isolated from wild-type and permissive temperature grown *erv1-101* and *mia40-3* strains. The import of Su9-DHFR was followed as Erv1-Mia40-independent import control. *p*, precursor; *m*, mature. In the bar graphs, the bands in the *right panel* were quantified using the histogram function of the Adobe Photoshop program and expressed as percentages of WT values. *B* and *C*, reconstitution of Cmc1 oxidative folding following 4 h of incubation and subsequent analysis of AMS-trapped thiols (*B*) or  $\text{H}_2\text{O}_2$  production (*C*, fluorometric Amplex Red assay). *D*, formation of intermolecular disulfides involving Cmc1, Mia40, and Erv1.

3-min incubation at 25 °C, import reactions were initiated by the addition of 5–10  $\mu\text{l}$  of translation mix. Aliquots were removed at fixed intervals during the reaction time course, and import was terminated with either cold buffer, protease (25  $\mu\text{g}/\text{ml}$  trypsin or 0.3 mg/ml proteinase K (PK)) or a combination of both. If trypsin was added to digest nonimported precursor protein, soybean trypsin inhibitor was subsequently added in excess after 15 min of incubation on ice. If PK was used, 1 mM PMSF was added in excess after 30 min of incubation on ice. After a final recovery by centrifugation (8,000  $\times g$ , 5 min), mitochondria were disrupted in Laemmli sample buffer. Samples from import reaction time points were resolved by SDS-PAGE, and gels were dried prior to exposing to film.

**Pulldown of *in Organello* Imported Radiolabeled Proteins**—Coimmunoprecipitation experiments following *in organello* protein import were performed as reported (21). Briefly, following import of  $^{35}\text{S}$ -labeled proteins into mitochondria or mitoplasts (prepared by hypotonic swelling of mitochondria), the reaction was stopped by the addition of 50 mM iodoacetamide. Mitochondria/mitoplasts were isolated and solubilized for 20 min on ice in a buffer containing 1% digitonin, 20 mM Tris-Cl, pH 7.4, 50 mM NaCl, 10% (w/v) glycerol, and 50 mM iodoacetamide. After clarification of the solubilized material, supernatants were collected and incubated with specific antibodies coupled to protein A-Sepharose beads for 1 h at 4 °C. Preimmune serum was used as a negative control. Antibody-bound material was washed three times in digitonin containing buffer. The samples were supplemented with Laemmli buffer, heated at 95 °C for 5 min, and analyzed by SDS-PAGE.

## RESULTS

**Cmc1 Is a substrate of the Mia40 Import Pathway**—The twin  $\text{CX}_2\text{C}$  motifs in Cmc1 predict that it is a substrate of the Mia40 import pathway. This was tested by *in organello* import assays of *in vitro* synthesized  $^{35}\text{S}$ -radiolabeled precursor Cmc1. We used mitochondria isolated from wild-type, *ts erv1-101* (17) and *mia40-3* (2) yeast mutant strains, in which import through the Mia40-Erv1 pathway is already compromised at the permissive temperature (Fig. 1A). At this temperature, the import efficiency of Cmc1 into *erv1-101* and particularly *mia40-3* relative to wild-type mitochondria was markedly decreased (Fig. 1A). As a control for Mia40-Erv1-independent import, dihydrofolate reductase carrying an ATPase subunit 9 targeting sequence (Su9-DHFR) was well imported into wild-type, *erv1-101*, and *mia40-3* mitochondria. A mitochondrial membrane potential ( $\Delta\Psi$ ) was not essential for Cmc1 import (not shown). Taken together, these data indicate that Cmc1 is a Mia40 import substrate. To further analyze Cmc1 oxidation, we fully reconstituted the import system *in vitro* by incubation of recombinant reduced Cmc1 with Erv1 and Mia40 in molar concentrations of 5:1:1 for 4 h as reported (10), at which time the oxidation of Cmc1 was analyzed by thiol trapping with AMS.

In control reactions, Cmc1 was shown to be fully reduced at the start of the experiment and did not become spontaneously oxidized after up to 4 h (Fig. 1B). In contrast, Cmc1 was partially oxidized in the presence of Erv1 (Fig. 1B). The incubation of Cmc1 with Mia40 resulted in a fraction of Cmc1 migrating as a higher molecular mass species, suggesting a stable interaction

with Mia40. The remaining Cmc1 not bound to Mia40 was not oxidized. The incubation of Cmc1 with both Erv1 and Mia40 resulted in an oxidized form of Cmc1. Because Cmc1 has one unpaired cysteine, only one AMS molecule was added, indicating the formation of two disulfide bonds. We refer to this species as fully oxidized Cmc1. A band corresponding to the size of a Cmc1 dimer was also detected. The Mia40-Cmc1 intermediate was apparently dissociated simultaneously with the full oxidation of Cmc1 by Mia40 and Erv1 (Fig. 1B). This suggested that Erv1 was needed for the release of Cmc1 from Mia40 and the oxidation of four cysteines in Cmc1.

To confirm that electrons from Cmc1 were transferred to Erv1 via Mia40, we performed a fluorometric Amplex Red assay, which measures the amount of H<sub>2</sub>O<sub>2</sub> produced during Cmc1 oxidation based on the reduction of oxygen by Erv1 (Fig. 1C). Reduced Cmc1, Mia40, or Erv1 generated only minimal amounts of H<sub>2</sub>O<sub>2</sub> when incubated alone. In addition, incubation of reduced Cmc1 with Mia40 also led to a negligible amount of H<sub>2</sub>O<sub>2</sub> being produced, whereas incubation with Erv1 resulted in marginal H<sub>2</sub>O<sub>2</sub> production. This suggests that the oxidation of Cmc1 by Erv1 occurs at a slow rate. A substantial amount of H<sub>2</sub>O<sub>2</sub> was generated only when Cmc1 was oxidized in the presence of both Mia40 and Erv1, showing that Cmc1 participates in a disulfide relay with Mia40 and Erv1.

To verify that the high mobility band observed in the Cmc1 reconstitution in the presence of Mia40 alone was a *bona fide* Mia40-Cmc1 intermediate, we performed a reconstitution experiment in the absence of AMS and immunoblotted against Cmc1, Mia40, or Erv1. A high mobility intermediate band was detected with antibodies against either Cmc1 or Mia40 in the reaction mixture consisting of Cmc1 and Mia40 (Fig. 1D). No covalent interaction between Erv1 and Cmc1 was detected (Fig. 1D). The Mia40-Cmc1 stable intermediate interaction occurs through an intermolecular disulfide bond because addition of the reducing agent tris(2-carboxyethyl)phosphine disrupted the Mia40-Cmc1 interaction. Interestingly, tris(2-carboxyethyl)phosphine also disrupted dimeric (~26 kDa) and trimeric (~39 kDa) forms of Cmc1 (not shown).

Additional *in vitro* reconstitution of the import pathway was achieved by the inclusion of cytochrome *c* in our reconstitution protocol. This setting did not modify the results obtained with an excess of Cmc1, in that Erv1 and Mia40 are required for full Cmc1 oxidation, which was accomplished in ~15 min (not shown). However, we opted not to include cytochrome *c* in most of our experiments because we detected substrate oxidation when incubated beyond 20–30 min in the presence of only cytochrome *c* (not shown).

**Cmc1 Is Oxidized *In Vitro* by Excess of Mia40**—Because excess Mia40 alone is able to fully oxidize Cox19 (20), we have tested the Mia40 dosage effect on the formation of the Mia40-Cmc1 intermediate and Cmc1 oxidation. When Mia40 was present in 5- or 20-fold excess, a fraction of Cmc1 was completely oxidized without requiring the presence of Erv1 (Fig. 2). However, a large fraction remained trapped within the Mia40 intermediate even after 30 min of incubation (Fig. 2).

**Cmc1 Is a Substrate of Erv1 *In Vitro***—We have further analyzed the intriguing ability of Erv1 to directly oxidize Cmc1 *in vitro*. We determined that, in a time-dependent manner, the

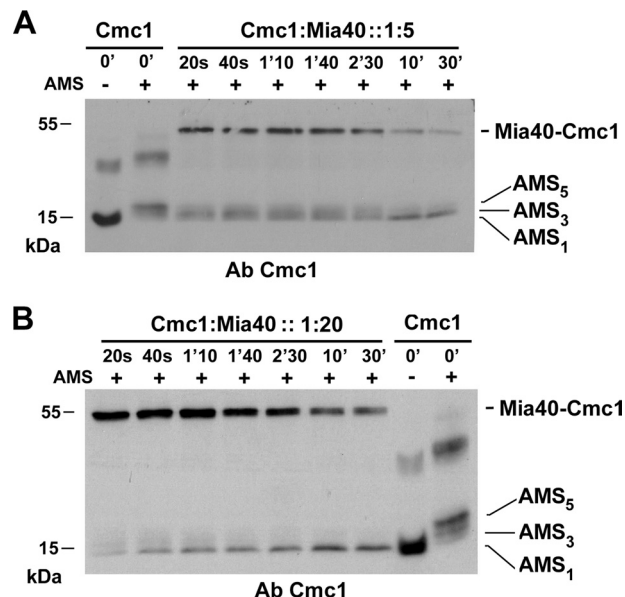


FIGURE 2. Cmc1 can be fully oxidized *in vitro* by Mia40 alone. Reconstitution time course with reduced Cmc1 alone or incubated with either 5- (A) or 20-fold (B) excess of Mia40 followed by analysis of AMS-trapped thiols by nonreducing SDS-PAGE.

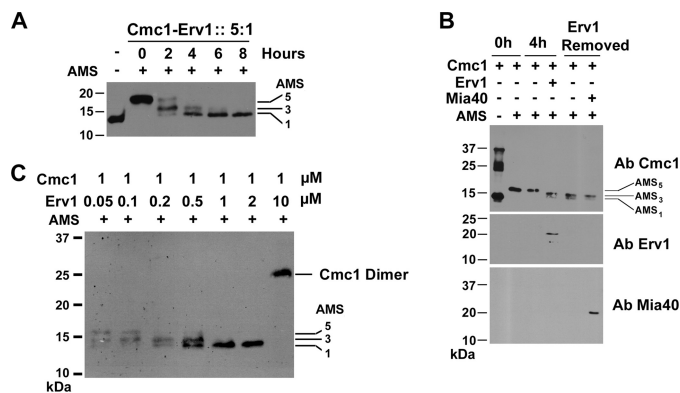


FIGURE 3. Cmc1 is an *in vitro* substrate of Erv1. A, time course of oxidation of reduced Cmc1 by Erv1. B, effect of Mia40 in Cmc1 partially oxidized by Erv1. Reduced Cmc1 was mixed with Erv1 for 4 h. Next, Erv1 was removed by His tag affinity cobalt beads. The Erv1-free sample was then incubated with or without Mia40 for 2 h. C, titration of Erv1 with Cmc1 held constant at 1 μM. In A–C, the samples were treated as in Fig. 1.

presence of Erv1 in substoichiometric amounts can progressively, albeit slowly, oxidize Cmc1 from a reduced state to a partially oxidized state and finally to a fully oxidized state (Fig. 3A).

We examined the order of protein oxidation/folding by following Cmc1 oxidation after incubation with Erv1 for 4 h prior to removal of Erv1 with His tag affinity cobalt beads. Subsequently, we incubated partially oxidized Cmc1 in the presence or absence of Mia40 for an additional 2 h. The incubation with Erv1 first resulted in the partial oxidation of Cmc1 (Fig. 3B). The removal of Erv1 and subsequent incubation with and without Mia40 resulted in no further oxidation of Cmc1. In addition, no Mia40-Cmc1 intermediate was detected, suggesting that the Mia40-Cmc1 interaction could not occur with the partially oxidized Cmc1 (Fig. 3B). Incubation of Cmc1 with increasing concentrations of Erv1 for 4 h resulted in a propor-

## Oxidative Folding of Cmc1

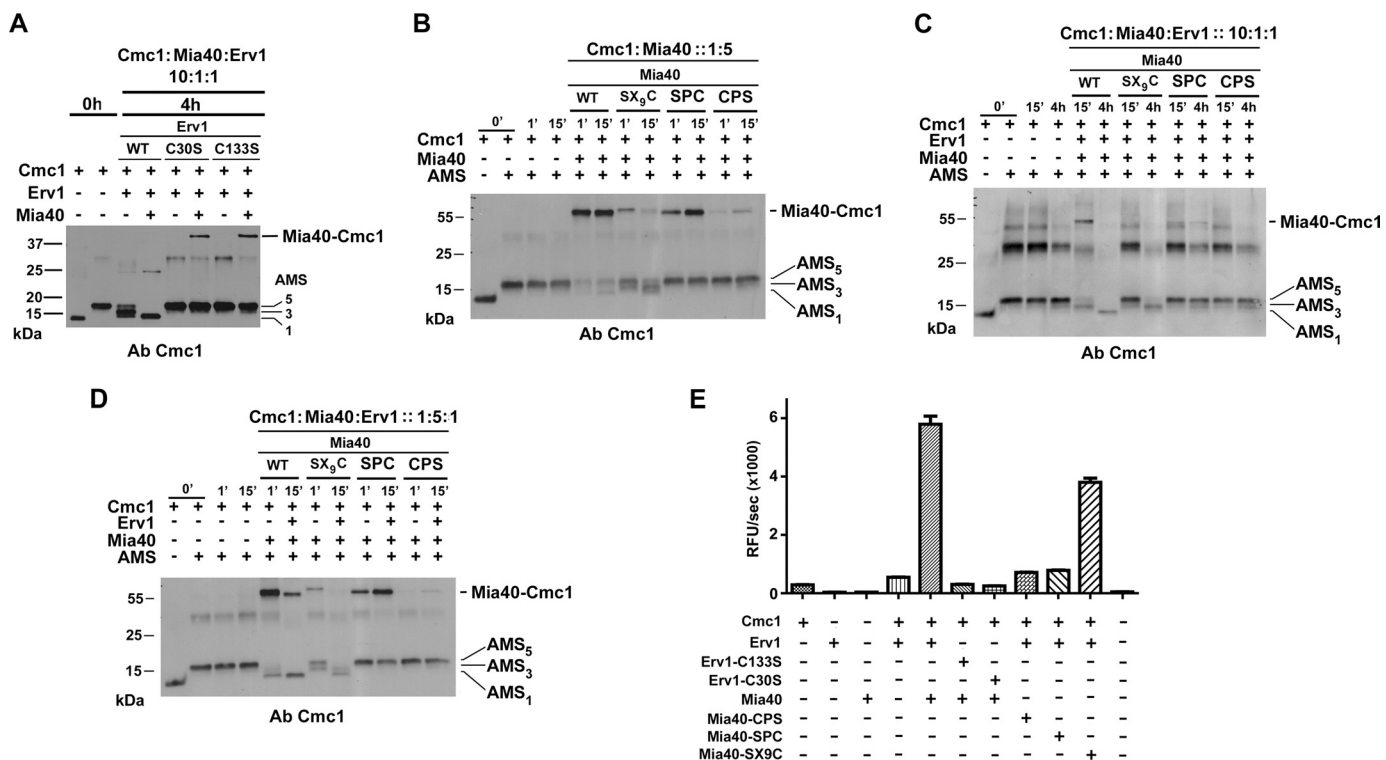


FIGURE 4. Cmc1 interacts with the second cysteine of the CPC active site of Mia40, and release from Mia40 requires a functional Erv1 protein. A, reconstitution of Cmc1 oxidative folding following 4 h of incubation and analysis of AMS-trapped thiols using wild-type, C30S, and C133S Erv1 purified protein in the presence and absence of Mia40. The first line includes Cmc1 alone without AMS; all of the other samples contain AMS. B–D, reconstitution of Cmc1 oxidative folding and analysis of AMS-trapped thiols using wild-type, SX<sub>9</sub>C, SPC, and CPS purified Mia40 protein in the presence and absence of Erv1 in the indicated stoichiometries. E, fluorometric Amplex Red assay performed as in Fig. 1C with mutant forms of Erv1 and Mia40.

tionally increased rate of Cmc1 oxidation, being complete at a 1:1 molar ratio (Fig. 3C).

The kinetics of Cmc1 oxidation by Erv1 *in vitro* is certainly slow, and it seems plausible that *in vivo* it could take place at a post-import stage. At this point we can only speculate that such a role could be relevant to Cmc1 roles in mitochondrial biogenesis (8, 23) and will be the subject of future studies.

When Cmc1 was incubated with Erv1 at a 10-fold excess, all Cmc1 was oxidized and formed a dimer (Fig. 3C). We have also observed dimerization of a very small portion of Cmc1 in *in organello* import assays (see Fig. 7). To determine whether Cmc1 exists as a dimer *in vivo*, we have engineered wild-type and  $\Delta$ cmc1 strains carrying integrative constructs expressing Cmc1–3×HA, Cmc1–9×Myc, or both. Using these strains in reciprocal pulldown assays, we failed to copurify both Cmc1-tagged versions or a tagged and a nontagged CMC1 version in the corresponding strains (not shown). These results indicate that Cmc1 does not exist as a stable homodimer *in vivo*, although we cannot discard the existence of transient homodimerization as an aspect of Cmc1 metabolism.

**A Functional Erv1 Is Required for Cmc1 Release from Mia40 and for Direct Oxidation of Cmc1**—To determine whether a functional Erv1 was needed for Mia40 recycling and the release of Cmc1 from Mia40 and Cmc1 oxidation, we performed reconstitution assays using Erv1 mutants in a Cmc1:Mia40: Erv1 stoichiometry of 5:1:1. Erv1 contains six cysteines that form three pairs. We used two Erv1 mutants of redox-active cysteines C30S and C133S. Cys-30 is part of the “shuttle” pair of

redox active cysteines because it is involved in shuttling electrons from the substrate to the active site cysteine pair, which includes Cys-133. The last cysteine pair performs a structural role (11, 25). Cmc1 was fully reduced at the beginning of the experiment, partially oxidized in the presence of Erv1, and fully oxidized in the presence of wild-type Erv1 and Mia40 (Fig. 4A). In contrast, Erv1 mutants were unable to partially oxidize Cmc1 directly. The Erv1 mutants were also unable to aid in the oxidation of Cmc1 when incubated in the presence of Mia40 (Fig. 4A), and Cmc1 remained trapped in the Mia40-Cmc1 complex, confirming the necessity of a functional Erv1.

**Cmc1 Binds to the Second Cysteine in the CPC Active Site of Mia40 and Disulfide Bond Formation between the Cysteines of the CPC Motif Is Required for Cmc1 Release**—To further examine the interaction between Cmc1 and key cysteine residues of Mia40, we performed Cmc1 reconstitution assays with purified Mia40 mutants. Mia40 contains four cysteines in a twin CX<sub>9</sub>C motif that is necessary for structural stability of the protein. Mutations in these cysteines result in decreased functional activity of Mia40. Two additional cysteines are part of the active site CPC motif. Mutations of either CPC cysteines result in loss of Mia40 activity (10, 26). Neither wild-type nor several Mia40 cysteine mutants were able to directly oxidize Cmc1 when present in substoichiometric concentrations (not shown). When Mia40 was in excess (Fig. 4B) or in the combined presence of Erv1 (Fig. 4, C–E), the substitution to a serine of the first cysteine (Cys-307) in the twin CX<sub>9</sub>C motif of Mia40 did not prevent Cmc1 oxidation, although the Cmc1-Mia40 intermediate

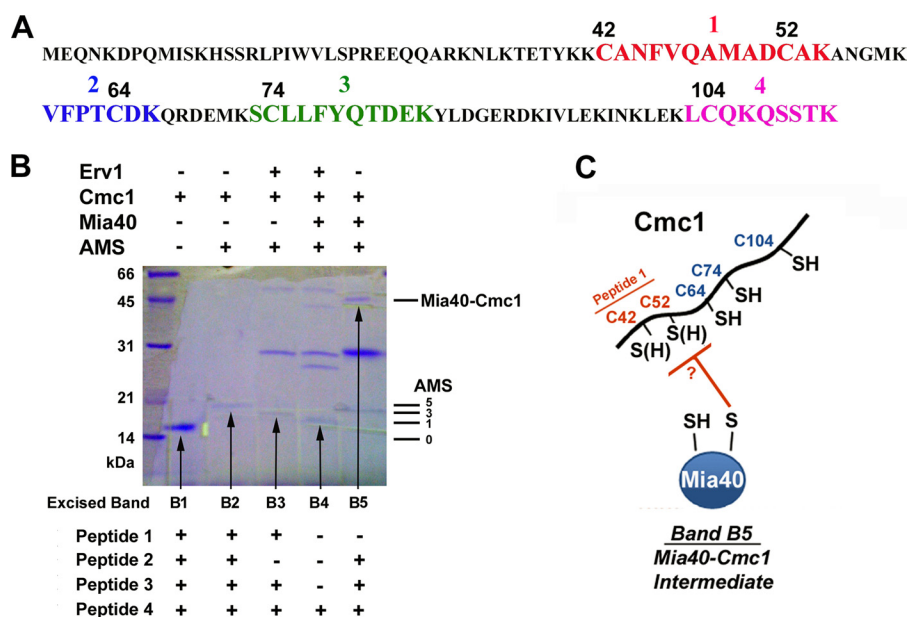


**FIGURE 5. Identification of disulfide bonds by mass spectrometry.** *A*, amino acid sequence of Cmc1. Tryptic peptides 1–4, which contain cysteines, are highlighted. *B*, Coomassie-stained gel of varying states of Cmc1 oxidation. The bands were excised from the gel and sent for mass spectrometry analysis. The excised bands include: band 1 (*B1*), fully reduced and unmodified Cmc1; band 2 (*B2*), fully reduced and AMS-modified Cmc1; band 3 (*B3*), partially oxidized and AMS-modified Cmc1; band 4 (*B4*), fully oxidized and AMS-modified Cmc1; and band 5 (*B5*), Mia40-Cmc1 intermediate. Below the gel are indications of the presence or absence of modified cysteine-containing peptides as indicated in *A*. Note that for excised band 1, the unmodified versions of the peptides were detected. *C*, model presenting the cysteine residues involved in the Mia40-Cmc1 interaction in band 5 in *B*.

was less stable than for the wild-type protein and barely detected even after 15 min of incubation time (Fig. 4, *C* and *D*). When the first cysteine in the Mia40 CPC motif was mutated to a serine (SPC), Cmc1 was still able to form an intermediate with Mia40. This intermediate, however, was not disrupted even in the presence of Erv1, and no oxidation of Cmc1 was observed (Fig. 4, *C* and *D*), thus suggesting that Erv1 oxidized Mia40, although not discarding it could act also on the substrate. Mutation of the second cysteine in the CPC motif (CPS) largely blocked formation of the Mia40-Cmc1 intermediate, and Cmc1 remained reduced (Fig. 4, *C* and *D*). The ability of the SPC mutant in the active site reactive disulfide motif to form the Mia40-Cmc1 intermediate can be explained by the fact that this mutant protein is known to form intermolecular disulfide-bonded dimers *in vitro* and *in vivo*, and thus this intermolecular disulfide bond can act as the catalytic site (27). These results suggest that the second cysteine of the CPC motif in Mia40 is involved in the intermolecular disulfide bond between Mia40 and Cmc1 and that a disulfide bond must be formed between the cysteines of the CPC motif of Mia40 to release Cmc1. The results obtained from the *in vitro* reconstitution assays with Erv1 and Mia40 mutants in substoichiometric concentrations were consistent with results obtained by the fluorometric Amplex Red assay to measure Cmc1 oxidation as indicated by H<sub>2</sub>O<sub>2</sub> produced during the reduction of O<sub>2</sub> by Erv1 (Fig. 4*E*).

To further examine the folding state of Cmc1 within the Mia40-Cmc1 intermediate, we performed the reconstitution assay (Cmc1:Erv1:Mia40 at 5:1:1) with AMS addition followed by nonreducing SDS-PAGE and Coomassie Blue staining. Several bands were excised from the gel (Fig. 5*B*) and analyzed by mass spectrometry. The analyzed bands were: B1, unmodified reduced Cmc1; B2, AMS-modified reduced Cmc1; B3, partially oxidized Cmc1 by Erv1; B4, fully oxidized Cmc1 by Mia40 and

Erv1; and B5, Mia40-Cmc1 intermediate. Mass spectrometry analysis was able to identify the five cysteines of Cmc1 that were modified within four tryptic peptide fragments (Fig. 5*A*). Peptide 1 contains cysteines Cys-42 and Cys-52. Peptides 2, 3, and 4 contain single cysteine residues Cys-64, Cys-74, and Cys-104, respectively. Mass spectrometry analysis reveals the addition of AMS to a reduced cysteine because the ions detected are 510 daltons larger for each modified cysteine than what would be predicted for the same ions in an unmodified peptide (not shown and Ref. 28). The pattern of detectable AMS-modified cysteine-containing peptides differed for each excised band. All peptides were observed in bands B1 (unmodified) and B2 (with AMS additions). The absence of peptide 2 in B3 was surprising. We would have expected that if C64 was involved in a disulfide bond to C52, then peptides 1 and 2 would be absent in band B3. The presence of peptides 1, 3, and 4 and the absence of peptide 2 indicates that peptide 2 is involved in a mix of disulfide bonds with cysteines in peptides 1, 3, or 4. These results suggest that during the oxidative folding of Cmc1 by Erv1, aberrant oxidative states may occur and that these states are probably minimized in a mechanism that would require the coordinate action of Mia40 and Erv1. Concerning band B4, only peptide 4 was detected, thus indicating that Cys-104 is not involved in disulfide bond formation. Band B5 did not reveal peptide 1, indicating that Cys-42 or Cys-52 is involved in formation of the Mia40-Cmc1 intermediate (Fig. 5, *B* and *C*). These patterns also support the conclusion that in the Cmc1-Mia40 intermediate, no intramolecular disulfides are formed in Cmc1 and that Cmc1 native oxidative folding requires additional oxidized Mia40 molecules or the action of Erv1.

*Cmc1 Oxidative Folding by Mia40 and Erv1 Is Specific for the Wild-type Protein*—To study the relevance of the cysteines present in Cmc1 for protein import, stability, and function, we

## Oxidative Folding of Cmc1

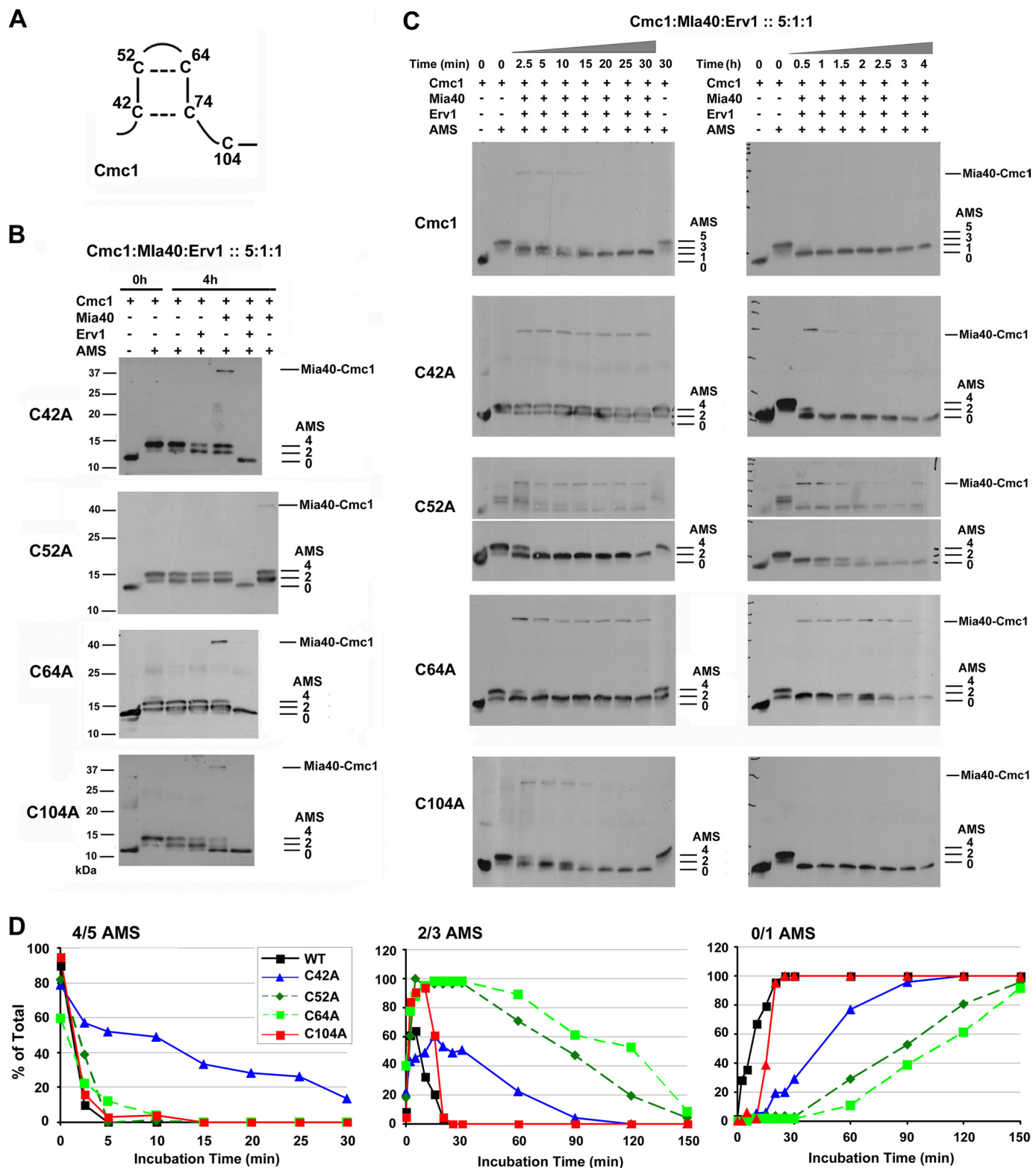


**FIGURE 6. Folding requirements and oxidized kinetics are altered in Cmc1 cysteine mutant variants.** *A*, schematic diagram of Cmc1 showing the cysteine residues in a hypothetical folding based on the structure of other CX<sub>2</sub>C proteins. *B*, reconstitution of oxidative folding and analysis of AMS-trapped thiols using Cmc1 cysteine mutants. *C*, reconstitution of wild-type and mutant variants of Cmc1 oxidative folding with Mia40 and Erv1 (molar ratio, 5:1:1) following time course incubations up to 4 h as indicated and subsequent analysis of AMS-trapped thiols. *D*, the bands for the reconstitution assays in *C* corresponding to fully reduced (4/5 AMS), partially oxidized (2/3 AMS), and fully oxidized (0/1 AMS) Cmc1 were quantified using the histogram function of the Adobe Photoshop program and expressed as percentages of total signal at each time point for each protein (WT or mutant Cmc1).

performed mutagenesis studies by changing each cysteine to alanine (Fig. 6A). First, we aimed to explore how the cysteine mutations in Cmc1 affected the requirement of Mia40 and Erv1

for the full oxidation of each variant, and second, we wanted to test whether they affected the formation of the Mia40-Cmc1 intermediate *in vitro*. When we examined the reconstitution of



the C42A mutant, we found that although the protein did not spontaneously oxidize, it was partially oxidized by either Erv1 or Mia40 alone. However, incubation of the C42A mutant protein with both Erv1 and Mia40 was required for full oxidation of the Cmc1 variant (Fig. 6B). The C52A and C64A mutant proteins proved to be challenging to purify and reduce. It was clear, however, that the portion of the purified C52A and C64A proteins that was reduced required the presence of both Erv1 and Mia40 for a full oxidation (Fig. 6B). Finally, we examined the reconstitution of the C104A mutant protein. C104A can spontaneously become oxidized, and this oxidation is enhanced by Erv1. Interestingly, full oxidation of C104A occurs not only in the combined presence of Mia40 and Erv1 but also extensively by Mia40 alone (Fig. 6B). This suggested that the fifth cysteine was important in controlling Cmc1 oxidation.

In the reconstitution assays, one would expect the kinetics of nonphysiological disulfide bond formation in the C42A, C52A, and C64A mutants to be different from that of the wild-type Cmc1 protein. This was tested by time course reconstitution assays of the Cmc1 variants in the presence of both Erv1 and Mia40 in the proportion 5:1:1. In these conditions, wild-type Cmc1 and C104A were fully oxidized after 15 min (Fig. 6, C and D). On the contrary, full oxidation of C42A, C52A, and C64A proceeded at a significantly slower rate. For C42A, the first disulfide bond is formed in 25–30 min, and the second is formed readily after the first. For C64A and C52A, the first disulfide is formed in 10 min, but ~2 h are required for the second disulfide to be formed (Fig. 6, C and D). These results support the concept of specificity for the Cmc1 import mechanism involving Mia40 and Erv1 and support that in the absence of key cysteines, aberrant disulfides can form although with kinetics different from that of the wild-type protein. Importantly, in the reconstitution experiments we detected free Cmc1 forms with three (for wild type) or two (for cysteine variants) AMS molecules, suggesting that Cmc1 is released from Mia40 (or more precisely, their intermolecular disulfide is disrupted) following formation of the first disulfide (Fig. 6, B and C).

The Mia40-Cmc1 intermediate was formed in the reconstitution of all four Cmc1 mutants with Mia40 (Fig. 6, B and C), as it was formed during *in organello* import assays (Fig. 7). The fact that the formation of the first disulfide bond in the reconstitution of Cmc1 C42A was markedly slow (Fig. 6D) is consistent with a role for Cys-42 in the formation of the native disulfide bond between Mia40 and Cmc1. The intermediate is formed in the absence of Cys-42, with other cysteines forming a nonphysiological intermolecular disulfide with Mia40, which *in vitro* is disrupted only slowly.

**Cysteines in the Twin CX<sub>9</sub>C Motif of Cmc1 Are Important for Protein Import**—We have tested the *in vivo* role of Cmc1 cysteine residues. Cmc1 variants of each cysteine in the CX<sub>9</sub>C motifs were unable to complement the respiratory growth defect of a yeast  $\Delta$ cmc1 strain even when overexpressed (Fig. 7A). In contrast, the C104A mutation did not affect respiratory growth (Fig. 7A). Isolated mitochondria from these strains were analyzed by Western blot for the steady state levels of Cmc1. Cmc1 mutants of Cys-104 accumulate in mitochondria at levels similar to that of wild-type, and the C64A mutant accumulate at

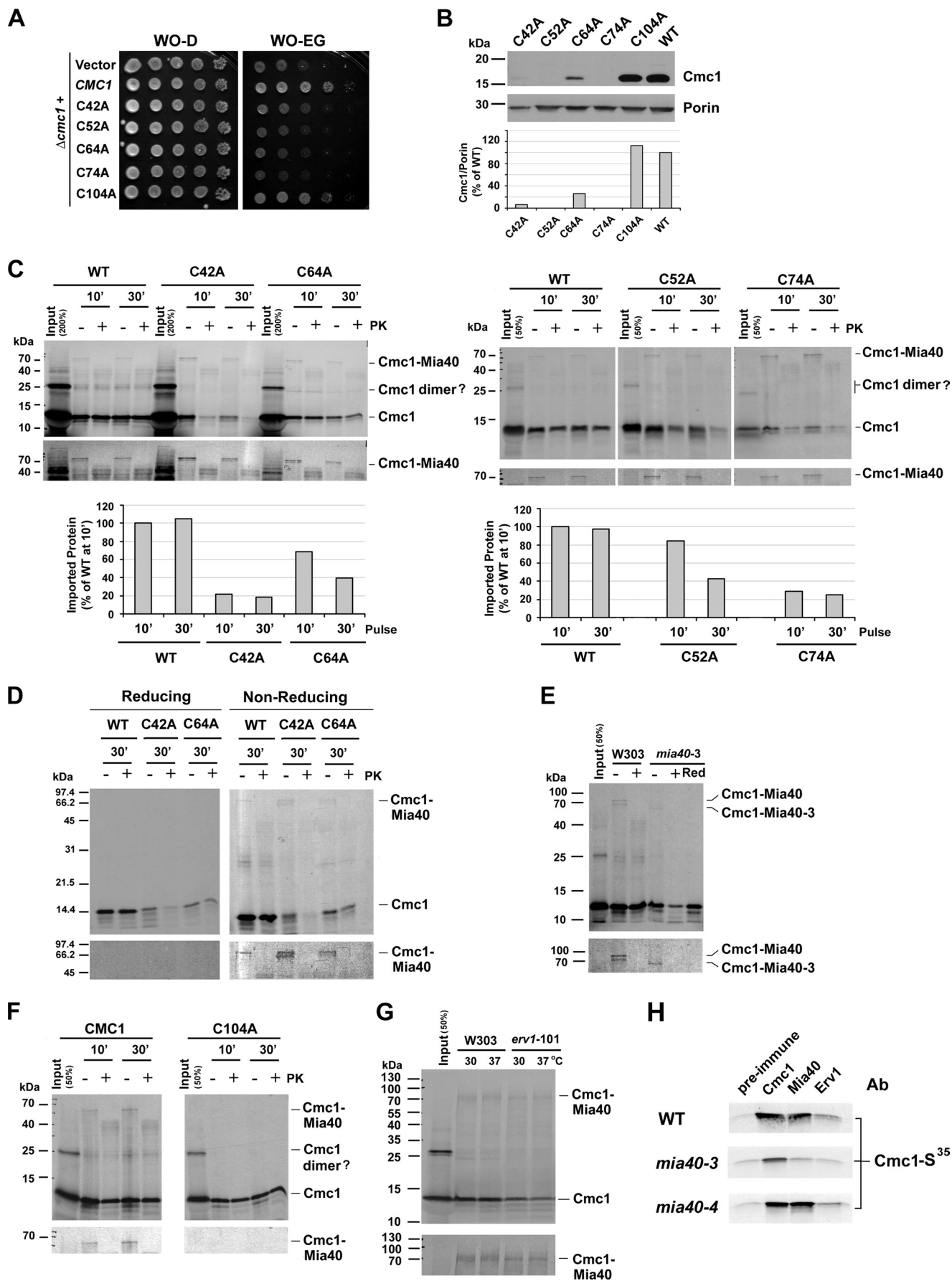
levels significantly lower (Fig. 7B). The mutants C42A, C52A, and C74A were barely detected even when the film was overexposed. This could be due either to the lack of import of the protein or to the poor stability and enhanced turnover of the protein.

To determine which scenario was occurring, we performed *in organello* import assays. Import of radiolabeled wild-type and C64A mutant was robust into wild-type mitochondria, although the mutant protein was not stable during the time of the experiment (Fig. 7C). The import of Cmc1 C52A followed the same kinetics pattern as import of the C64A variant, albeit with less efficiency than the import of wild-type Cmc1. Import of Cmc1 C42A and C74S was instead very poor (Fig. 7B). This agrees with the *in vivo* data and suggests that the four cysteines in the CX<sub>9</sub>C motifs are important for the import or the stability of the protein. Cys-42 and Cys-74 are essential for import of Cmc1, whereas Cys-64 and Cys-52 are important for its stability. Taken together with the mass spectrometry data, these results would suggest that Cys-42, the first cysteine of the CX<sub>9</sub>C motif, is the one interacting with Mia40 in the Mia40-Cmc1 intermediate, similar to what has been observed for the Tim9 and Tim10 substrates (13, 14). Notably, in our import assays were evident two faint bands of sizes compatible with that of a Cmc1 dimer and of the Cmc1-Mia40 intermediate. These bands were sensitive to reducing conditions (Fig. 7, C and D), thus suggesting the existence of intermolecular disulfide bridges. The Cmc1-Mia40 band was detected when using wild-type, C42A, C52A, C64A, and C74A Cmc1 (Fig. 7C), indicating that the intermediate can be formed in the absence of any of these cysteines, although it does not allow for an efficient import of C42A Cmc1. We observed that the intermediate was sensitive to PK digestion, which would indicate that when Cmc1 interacts with Mia40, a portion of Cmc1 remains exposed to PK (Fig. 7, C and D). However, the intermediate was not sensitive to trypsin digestion for reasons that we do not fully understand (not shown). To further confirm the nature of the intermediate, we analyzed its formation during the import of wild-type Cmc1 into *mia40-3* mitochondria. In this strain, Mia40 is of a smaller size because of a C-terminal truncation, and its function is temperature-sensitive (2). Using *mia40-3* mitochondria, we detected a high molecular mass band migrating faster than the Cmc1-Mia40 wild-type intermediate. This is consistent with a Cmc1-Mia40-3 intermediate because of the C-terminal truncation of Mia40-3 (Fig. 7E), thus confirming the formation of the Cmc1-Mia40 intermediate during *in organello* import of Cmc1.

Finally, we noticed that *in organello* import of the Cmc1 variant missing the unpaired Cys-104 cysteine seems to be more efficient than import of wild-type Cmc1, consistently showing fast and complete resolution of the Cmc1-Mia40 intermediate (Fig. 7F). The presence of Cys-104 could increase the chances of nonphysiological disulfide formation whose resolution would delay the correct protein oxidative folding.

**Cmc1 Forms a Ternary Complex with Mia40 and Erv1**—Because Erv1 is necessary for the release of Cmc1 from the heterodimeric complex with Mia40 when the latter is not in excess, we could expect the three proteins to form a ternary complex during the reaction of substrate oxidation. However, this intermediate is most probably short-lived and difficult to detect *in vivo*.

# Oxidative Folding of Cmc1



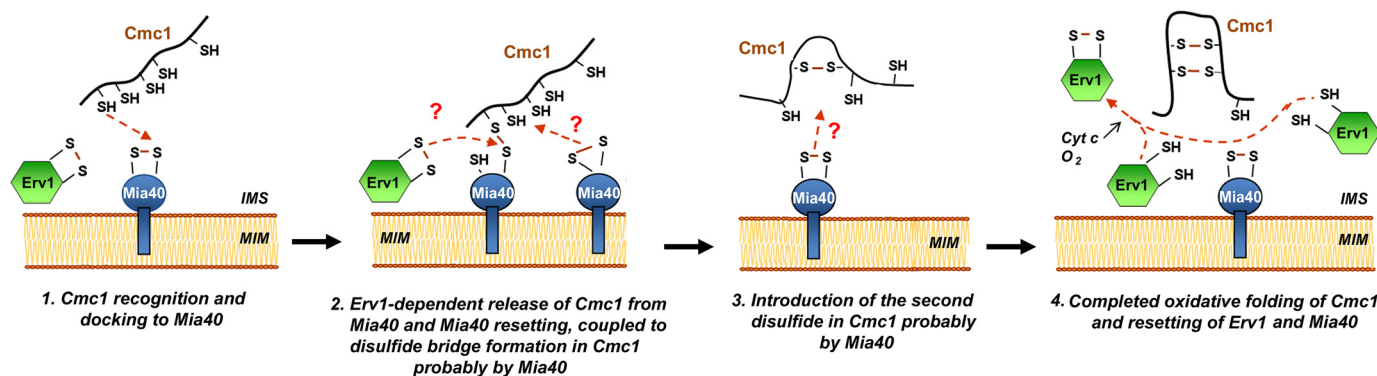


FIGURE 8. **Model of Cmc1 oxidative folding in the mitochondrial IMS.** See explanation under "Discussion." For simplification, a possible role of Erv1 in substrate oxidation in steps 2 and 3 is not depicted.

Working with the *in organello* import system, we showed that in the absence of a completely functional Erv1 in mitochondria isolated from an *erv1 ts* mutant (*erv1-101*), Cmc1 was not efficiently imported (Figs. 1A and 7G). However, there was an accumulation of the Mia40-Cmc1 intermediate at least similar to what was observed in wild-type cells using wild-type Cmc1 (not shown) and more prominently when using the C64A variant (Fig. 7G). These results further support the idea of Erv1 being required to resolve this intermediate *in vivo* and facilitate oxidative folding of Cmc1.

A ternary complex substrate-Mia40-Erv1, involving a small Tim protein, was previously detected by a combination of *in organello* import of radiolabeled protein followed by immunoprecipitation (21). The experiment was performed using mitoplasts isolated from cells expressing wild-type Mia40 or one of two *ts* reported variants (2), either Mia40-3, impaired in substrate binding, or Mia40-4, which efficiently binds substrate but is impaired in its release. In mitoplasts, the amount of Erv1 is reduced by 50%, which is known to slow down substrate oxidation and increase the accumulation of ternary intermediates (21). Radiolabeled Cmc1 imported into wild-type and *mia40-4* mitoplasts was immunoprecipitated with antibodies against Mia40, as well as Erv1, but not preimmune serum (Fig. 7H). In several repetitions, in wild-type and *mia40-4* mitoplasts, the anti-Erv1 pulldown signal was of an intensity 3–7-fold higher than with preimmune serum. To distinguish whether Cmc1 was directly coprecipitated with Erv1 or via binding to Mia40, we used the mutant form Mia40-3 as described (21). The pull-down was markedly attenuated when using *mia40-3* mitoplasts, and particularly in the Erv1 pulldown, we detected traces of radiolabeled Cmc1 of intensity similar to the preimmune serum (Fig. 7H). In mitoplasts, Cmc1 would have direct access

to Erv1 without a need for Mia40-dependent translocation across the outer membrane (13). This allowed us to conclude that Mia40 is required for the interaction of Erv1 with the Cmc1 substrate.

## DISCUSSION

Import of several cysteine-rich proteins into the mitochondrial IMS proceeds via the Mia40 import pathway, which ensures the oxidative folding of its substrates. Here, we have analyzed the import and oxidative folding of Cmc1 and have determined the role its cysteines play in these processes.

Cmc1 contains four cysteines as part of a twin CX<sub>2</sub>C motif with an additional fifth cysteine near the C terminus (23). The evidence provided in this study allows us to predict the sequence of events that occur during mitochondrial import and oxidative folding of proteins such as Cmc1 (Fig. 8). First, the newly imported substrate (e.g., Cmc1) recognizes and creates an intermolecular disulfide bond with the second cysteine in the active site of Mia40, similar to that reported for the small Tim proteins (11). Second, Erv1 transiently interacts with the Mia40-Cmc1 complex and facilitates the oxidative folding of Cmc1 by forming an intramolecular disulfide bond in Mia40, which is coupled to formation of a disulfide bond in Cmc1 and the release of folded Cmc1 from the complex. Although Mia40 can fully oxidize Cmc1 *in vitro*, a possible action of Erv1 on the substrate has not been fully eliminated as discussed later. Finally, this initial disulfide bond presumably induces a conformational change to Cmc1, which subsequently could likely allow Mia40 to catalyze the second disulfide bond formation, although a role for Erv1 in this step has not been ruled out. Eventually, reduced Erv1 would interact with oxygen or cytochrome *c*, thus becoming oxidized (17–19).

FIGURE 7. **Importance of the CX<sub>2</sub>C cysteines for Cmc1 import by Mia40 and Erv1.** A, *in vivo* yeast complementation of a  $\Delta cmc1$  strain with overexpressed cysteine to alanine Cmc1 variants. Serial dilutions were spotted on solid synthetic media containing dextrose (WO-D) or ethanol-glycerol (WO-EG). Pictures were taken after 2 and 4 days of incubation at 30 °C. B, steady state levels of Cmc1 in mitochondria isolated from a  $\Delta cmc1$  mutant strain overexpressing each Cmc1 variant. Porin was used as a loading control. The bands in the upper panel were quantified using the histogram function of the Adobe Photoshop program and expressed as percentages of WT values. C, *in organello* import of <sup>35</sup>S-labeled WT, C42A, C52A, C64A, and C74A Cmc1 into wild-type mitochondria. The proteins were separated by nonreducing SDS-PAGE. The signals were quantified as in B and expressed as percentages of WT values. D, same as in C, but the proteins were separated by both reducing and nonreducing SDS-PAGE. E, *in organello* import of <sup>35</sup>S-labeled wild-type Cmc1 into wild-type and *mia40-3* mitochondria. The proteins were separated by nonreducing PAGE except the sample labeled as Red, which was reducing. In C–E, the symbols + and – indicate treatment or not with PK. F, *in organello* import of <sup>35</sup>S-labeled wild-type and C104A Cmc1 into wild-type mitochondria. The proteins were separated by nonreducing SDS-PAGE. G, *in organello* import of Cmc1 C64A using wild-type and *erv1-101* mitochondria. The mitochondria were incubated for 15 min at either 30 or 37 °C prior to proceeding with the import reaction. Following import, the mitochondria were reisolated and left proteinase-untreated. In C–F, the lower panel is a longer exposition and more contrasted version of the higher molecular mass portion of the upper panel. H, following import of <sup>35</sup>S-labeled Cmc1 into WT, *mia40-3* or *mia40-4* mitoplasts, extracts were subjected to immunoprecipitation with the indicated antibodies.

## Oxidative Folding of Cmc1

We have aimed to identify the cysteine in Cmc1 involved in the intermolecular disulfide bond with Mia40. Our results showed that either the first (Cys-42) or second cysteine (Cys-52) of the CX<sub>2</sub>C motif in Cmc1 could play such a role, although we could not fully discriminate between them. Bioinformatics analyses for the presence of putative IMS-targeting/sorting signals (or mitochondrial intermembrane space sorting signal) in CX<sub>2</sub>C proteins have predicted Cys-52 as the docking cysteine in yeast Cmc1 (29). Somehow surprisingly, among 385 CX<sub>2</sub>C proteins across 20 different species analyzed in this study, the docking cysteine was found to be in the order first (39%) > third (37%) > fourth (20%) > second (4%) (29). This would be expected to have a significant impact on the mechanisms of folding and order of disulfide introduction for each individual protein. In the case of Cmc1, the IMS-targeting signal sequence is not conserved through evolution (not shown), thus questioning its relevance in this particular case. For Cmc1, the C42A and C52A variants are able to form an intermediate with Mia40 *in vitro* and *in organello*, although both cysteines are necessary for the accumulation of Cmc1 *in vivo* and for an efficient import *in organello*. However, a time course analysis of the *in vitro* folding of Cmc1 helped to clarify the roles of these cysteines. As with the wild-type protein, the C52 variant readily forms an intermediate with Mia40, which is promptly disrupted to yield a Cmc1 protein containing one disulfide, whereas the disruption of the Cmc1-Mia40 interaction and formation of the first disulfide in the Cys-42 variant proceeds very slowly. These results suggest that in agreement with previous observations with Tim substrates (13, 14), the first cysteine in the twin motif, Cys-42 in Cmc1, could be involved in the intramolecular disulfide with Mia40.

The folding of Cmc1 would be expected to occur in a sequential and specific fashion. Interestingly, reconstitution of the C42A, C52A, and C64A Cmc1 cysteine mutants resulted in unexpected oxidative states when incubated alone or in combination with Erv1 or Mia40 as compared with the wild type. The loss of cysteine residues probably forces the mutant proteins to oxidize/fold in such a way that mixed disulfides can form. This is also supported by the significantly slower rate of full oxidation of the C42A, C52A, and C64A variants by Erv1-Mia40 in our reconstitution experiments.

Among the four Cmc1 CX<sub>2</sub>C cysteine mutants, the most efficiently *in organello* and *in vivo* imported and stabilized variant is C64A. However, C64A is not functional and, similar to the other three variants, it was unable to complement the respiratory defect of  $\Delta cmc1$  yeast cells. On the contrary, the C104A mutant, which affects an unpaired C-terminal cysteine, is imported as the wild-type protein, and the mutation does not affect the *in vivo* function of Cmc1. Noticeably, the Cmc1 Cys-104 was imported *in organello* apparently more efficiently than the wild-type protein as indicated by the poor accumulation of the Cmc1 Cys-104-Mia40 intermediate. The presence of unpaired cysteines in CX<sub>2</sub>C substrates like Cmc1 probably increases the likelihood of nonphysiological disulfide formation whose resolution would be expected to delay their correct oxidative folding. Seven of the 14 IMS localized twin CX<sub>2</sub>C proteins identified to date contain additional cysteines in addition to the four of the twin CX<sub>2</sub>C motif, which would suggest

the existence of a disulfide proofreading system, a role that glutathione was shown to be able to perform *in vitro* (20).

Whether Erv1 could play a role in import substrate oxidation *in vivo* has not been fully clarified. From an evolutionary perspective, the absence of Mia40 from trypanosomatids has suggested a model for stepwise evolution of the MIA pathway for import of cysteine-rich proteins (30). This model states that in early eukaryotes, the pathway was dependent upon Erv1 and that the subsequent evolution of Mia40 in providing a “receptor” for substrate recognition reflects a refinement of the import pathway that occurred at a later point in eukaryotic history. Erv1 could have acted as a substrate oxidase and perhaps collaborated with ancestral isomerase systems. Our data indicate that Mia40 is able to introduce two disulfides in Cmc1 *in vitro*. However, the possibility remains that *in vivo*, Erv1 could simultaneously oxidize Mia40 and the substrate, given that it is known to work as a functional dimer (20). We have shown that Erv1 alone was also able to slowly oxidize Cmc1 *in vitro*, although we speculate that *in vivo* this oxidation could take place at a post-import stage and perhaps could be relevant to Cmc1 roles in mitochondrial cytochrome *c* oxidase biogenesis (8, 23).

Here we have provided evidence for the existence *in organello* of a ternary Cmc1-Mia40-Erv1 complex. The twin CX<sub>2</sub>C-containing proteins Tim9 and Tim10 were also shown to form a ternary complex with Mia40 and Erv1 during import, and it was suggested that within the complex, sequential redox reactions would be spatially coupled, resulting in disulfide channeling (21). Our results with Cmc1 support the concept of channeling for disulfide transfer involving Mia40, Erv1, and CX<sub>2</sub>C substrates. This could be a strategy for the oxidative folding of twin CX<sub>2</sub>C proteins adapted to both facilitate efficient formation of multiple disulfides and prevent the formation of non-native disulfide bonds.

---

*Acknowledgments*—We thank Justin Hotter for technical support and Dr. Alejandro Ocampo for insightful discussion. We thank Dr. Brant Watson for critical reading of the manuscript.

---

## REFERENCES

1. Endo, T., and Yamano, K. (2009) Multiple pathways for mitochondrial protein traffic. *Biol. Chem.* **390**, 723–730
2. Chacinska, A., Pfannschmidt, S., Wiedemann, N., Kozjak, V., Sanjuán Szklarz, L. K., Schulze-Specking, A., Truscott, K. N., Guiard, B., Meisinger, C., and Pfanner, N. (2004) Essential role of Mia40 in import and assembly of mitochondrial intermembrane space proteins. *EMBO J.* **23**, 3735–3746
3. Naoé, M., Ohwa, Y., Ishikawa, D., Ohshima, C., Nishikawa, S., Yamamoto, H., and Endo, T. (2004) Identification of Tim40 that mediates protein sorting to the mitochondrial intermembrane space. *J. Biol. Chem.* **279**, 47815–47821
4. Mesecke, N., Terziyska, N., Kozany, C., Baumann, F., Neupert, W., Hell, K., and Herrmann, J. M. (2005) A disulfide relay system in the intermembrane space of mitochondria that mediates protein import. *Cell* **121**, 1059–1069
5. Herrmann, J. M., Kauff, F., and Neuhaus, H. E. (2009) Thiol oxidation in bacteria, mitochondria and chloroplasts: common principles but three unrelated machineries? *Biochim. Biophys. Acta* **1793**, 71–77
6. Riemer, J., Bulleid, N., and Herrmann, J. M. (2009) Disulfide formation in the ER and mitochondria: two solutions to a common process. *Science* **324**, 1284–1287

7. Longen, S., Bien, M., Bihlmaier, K., Kloeppe, C., Kauff, F., Hammermeister, M., Westermann, B., Herrmann, J. M., and Riemer, J. (2009) Systematic analysis of the twin CX<sub>9</sub>C protein family. *J. Mol. Biol.* **393**, 356–368
8. Horn, D., Zhou, W., Trevisson, E., Al-Ali, H., Harris, T. K., Salviati, L., and Barrientos, A. (2010) The conserved mitochondrial twin CX<sub>9</sub>C protein Cmc2 is a Cmc1 homologue essential for cytochrome c oxidase biogenesis. *J. Biol. Chem.* **285**, 15088–15099
9. Nobrega, M. P., Bandeira, S. C., Beers, J., and Tzagoloff, A. (2002) Characterization of COX19, a widely distributed gene required for expression of mitochondrial cytochrome oxidase. *J. Biol. Chem.* **277**, 40206–40211
10. Tienson, H. L., Dabir, D. V., Neal, S. E., Loo, R., Hasson, S. A., Boontheung, P., Kim, S. K., Loo, J. A., and Koehler, C. M. (2009) Reconstitution of the Mia40-Erv1 oxidative folding pathway for the small Tim proteins. *Mol. Biol. Cell* **20**, 3481–3490
11. Deponte, M., and Hell, K. (2009) Disulphide bond formation in the intermembrane space of mitochondria. *J. Biochem.* **146**, 599–608
12. Sideris, D. P., and Tokatlidis, K. (2010) Oxidative protein folding in the mitochondrial intermembrane space. *Antioxid. Redox Signal.* **13**, 1189–1204
13. Milenkovic, D., Gabriel, K., Guiard, B., Schulze-Specking, A., Pfanner, N., and Chacinska, A. (2007) Biogenesis of the essential Tim9-Tim10 chaperone complex of mitochondria. Site-specific recognition of cysteine residues by the intermembrane space receptor Mia40. *J. Biol. Chem.* **282**, 22472–22480
14. Sideris, D. P., and Tokatlidis, K. (2007) Oxidative folding of small Tims is mediated by site-specific docking onto Mia40 in the mitochondrial intermembrane space. *Mol. Microbiol.* **65**, 1360–1373
15. Grumbt, B., Stroobant, V., Terziyska, N., Israel, L., and Hell, K. (2007) Functional characterization of Mia40p, the central component of the disulfide relay system of the mitochondrial intermembrane space. *J. Biol. Chem.* **282**, 37461–37470
16. Banci, L., Bertini, I., Calderone, V., Cefaro, C., Ciofi-Baffoni, S., Gallo, A., Kallergi, E., Lionaki, E., Pozidis, C., and Tokatlidis, K. (2011) Molecular recognition and substrate mimicry drive the electron-transfer process between MIA40 and ALR. *Proc. Natl. Acad. Sci. U.S.A.* **108**, 4811–4816
17. Dabir, D. V., Leverich, E. P., Kim, S. K., Tsai, F. D., Hirasawa, M., Knaff, D. B., and Koehler, C. M. (2007) A role for cytochrome c and cytochrome c peroxidase in electron shuttling from Erv1. *EMBO J.* **26**, 4801–4811
18. Bihlmaier, K., Mesecke, N., Terziyska, N., Bien, M., Hell, K., and Herrmann, J. M. (2007) The disulfide relay system of mitochondria is connected to the respiratory chain. *J. Cell Biol.* **179**, 389–395
19. Allen, S., Balabanidou, V., Sideris, D. P., Lisowsky, T., and Tokatlidis, K. (2005) Erv1 mediates the Mia40-dependent protein import pathway and provides a functional link to the respiratory chain by shuttling electrons to cytochrome c. *J. Mol. Biol.* **353**, 937–944
20. Bien, M., Longen, S., Wagener, N., Chwalla, I., Herrmann, J. M., and Riemer, J. (2010) Mitochondrial disulfide bond formation is driven by inter-subunit electron transfer in Erv1 and proofread by glutathione. *Mol. Cell* **37**, 516–528
21. Stojanovski, D., Milenkovic, D., Müller, J. M., Gabriel, K., Schulze-Specking, A., Baker, M. J., Ryan, M. T., Guiard, B., Pfanner, N., and Chacinska, A. (2008) Mitochondrial protein import. Precursor oxidation in a ternary complex with disulfide carrier and sulfhydryl oxidase. *J. Cell Biol.* **183**, 195–202
22. Myers, A. M., Pape, L. K., and Tzagoloff, A. (1985) Mitochondrial protein synthesis is required for maintenance of intact mitochondrial genomes in *Saccharomyces cerevisiae*. *EMBO J.* **4**, 2087–2092
23. Horn, D., Al-Ali, H., and Barrientos, A. (2008) Cmc1p is a conserved mitochondrial twin CX<sub>9</sub>C protein involved in cytochrome c oxidase biogenesis. *Mol. Cell Biol.* **28**, 4354–4364
24. Stuart, R. A., and Koehler, C. M. (2007) *In vitro* analysis of yeast mitochondrial protein import, in *Current Protocols in Cell Biology*, Unit 11.19, John Wiley and Sons Eds, Somerset, NJ
25. Fass, D. (2008) The Erv family of sulfhydryl oxidases. *Biochim. Biophys. Acta* **1783**, 557–566
26. Terziyska, N., Grumbt, B., Kozany, C., and Hell, K. (2009) Structural and functional roles of the conserved cysteine residues of the redox-regulated import receptor Mia40 in the intermembrane space of mitochondria. *J. Biol. Chem.* **284**, 1353–1363
27. Banci, L., Bertini, I., Cefaro, C., Ciofi-Baffoni, S., Gallo, A., Martinelli, M., Sideris, D. P., Katrakili, N., and Tokatlidis, K. (2009) MIA40 is an oxidoreductase that catalyzes oxidative protein folding in mitochondria. *Nat. Struct. Mol. Biol.* **16**, 198–206
28. Tie, J. K., Jin, D. Y., Loisel, D. R., Pope, R. M., Straight, D. L., and Stafford, D. W. (2004) Chemical modification of cysteine residues is a misleading indicator of their status as active site residues in the vitamin K-dependent  $\gamma$ -glutamyl carboxylation reaction. *J. Biol. Chem.* **279**, 54079–54087
29. Cavallaro, G. (2010) Genome-wide analysis of eukaryotic twin CX<sub>9</sub>C proteins. *Mol. Biosyst.* **6**, 2459–2470
30. Allen, J. W., Ferguson, S. J., and Ginger, M. L. (2008) Distinctive biochemistry in the trypanosome mitochondrial intermembrane space suggests a model for stepwise evolution of the MIA pathway for import of cysteine-rich proteins. *FEBS Lett.* **582**, 2817–2825